ANTIFUNGAL ACTIVITY OF POLYETHYLENE GLYCOL COATED AND UNCOATED SILVER NANOPARTICLES, DERIVED FROM *KLEBSIELLA SPP*. AND NEEM LEAVES, AGAINST AZOLE RESISTANT *CANDIDA ALBICANS*.

Kunal Madhav[1], Archana Pandita[2]*, Garima Asthana[3], Kumar Saurav Singh[4].

Abstract:
The aim of the present study is to comparatively evaluate the antimicrobial effect of the silver nanoparticles, AgNPs, that were synthesized biogenically from the bacterial isolate *K. pneumoniae* (BNP) and Neem leaf extract (NLNP), for the best possible application as an alternative mode of treatment. The AgNPs thus formed were divided into 2 categories out which one part was capped with the Polyethylene glycol or PEG while the other part remained uncapped. These AgNPs were further characterized by TEM, UV-Vis Spectroscopy. FTIR, DLS and XRD in order to assess their molecular properties. Topographical assessment of size of these AgNPs by TEM demonstrated their size to be 19 nm for BNP and 24 nm for NLNP. These AgNPs were then tested for their antifungal activity against the azole resistant *C. albicans* that were obtained from the Chronic Periodontitis patients. Antimicrobial sensitivity testing of the isolated *C. albicans* demonstrated them to resist Fluconazole, Itraconazole, Clotrimazole and Ketoconazole group of antifungal antibiotics. Strong antimicrobial activity of BNP and NLNP against this pathogen was noted in the form of large zones of inhibition measuring 18.7 mm and 20.1 mm for NLNP and BNP, respectively. PEG coated NLNP on the other hand displayed 18 mm while PEG coated BNP displayed 18.2 mm of zone. Based on the study conducted it was observed that uncoated BNP had a strong antifungal activity on the azole resistant *C. albicans* as compared to the other AgNPs. The data thus obtained from the present study suggests that BNPs can be used as an alternative approach for the treatment of infections caused by Azole resistant *C. albicans*.

Keywords: Azole resistant, *C. albicans*, Polyethylene glycol, Capping, AgNP, Silver Nanoparticles, Period ontitis.

[1,2*]Dept. of Biotechnology, School of Engineering and Technology, Sharda University, Greater Noida, Uttar Pradesh.
[1]Dept. of Microbiology, I.T.S. Dental College, Hospital and Research Centre, Greater Noida, Uttar Pradesh.
[3,4]Dept. of Periodontology, I.T.S. Dental College, Hospital and Research Centre, Greater Noida, Uttar Pradesh.

***Corresponding Author:** Archana Pandita
*Dept. of Biotechnology, School of Engineering and Technology, Sharda University, Greater Noida, Uttar Pradesh.

DOI: - 10.48047/ecb/2023.12.si5a.079

1. Introduction:

Several pathogens tend to develop biofilms, which fulminates into various pathogenic conditions. Periodontitis is one of such conditions which involves various biofilm forming microorganisms that results in the inflammation of periodontium [1]. The inflammation is chronic in nature and is reported to cause infection of the supporting tissues around the teeth [2]. This condition is most often dominated by various group of microorganisms like *P. gingivalis, T. forsythia* and *T. denticola* [2]. Morphological changes attributed to this condition includes the demonstration of an irreversible destruction of soft and hard periodontal tissues, which forms a periodontal pocket [3]. Apart from the bacteria periodontal pocket, which harbors a wide variety of microorganisms including yeasts like *Candida* spp., is an opportunistic pathogen [4] that is involved in multiple oral complications including Periodontitis [5,6]. The virulence factors of *Candida* species facilitating their proliferation and colonization in the oral mucosa and periodontal pockets may also be responsible for invading the host defense by co-aggregating with the dental biofilm thereby contributing in the etiopathogenesis of periodontal disease by activation of the host immune response [1,7]. *Candida* produces enzymes like phospholipases, lipases, phospho-monoesterase, hexosaminidase, and aspartic proteinases, collagenases and proteases that degrade the extracellular matrix leading to progression of the disease [8–10]. Also, other factors including diversity in the phenotype, adhesion, formation of hyphae, production of virulence factors. Another aspect that could be held responsible for the pathogenicity of the *C. albicans* is its genetic constitution [11]. Various species like *C. dublineinsis, C. tropicalis. C. krusei* are present in the oral cavity [3,12,13] but *C. albicans* is most prevalent yeast found in the oral cavity in both healthy and diseased conditions displaying its pleomorphic nature [14,15].

Various medications have been prescribed for the treatment but till date use of oral Amphotericin B has proved to be effective against *C. albicans* followed by Fluconazole, Itraconazole, Nystatin [16,17]. Amongst these, antifungal antibiotics like Fluconazole, Ketoconazole and Itraconazole belongs to the family of the Azole group of antibiotics, which due to its high solubility in water and its high bioavailability makes it the most preferred drug of choice [18]. Azoles are also reported to inhibit the Ergosterol biosynthesis thereby inhibiting the fungal cell wall synthesis and promotes the formation of Reactive Oxygen Species or ROS [19,20]. In the recent times, emergence of several drug resistant forms of *C. albicans* have been reported making the situation complicated and thus leading to the poor diagnostics and treatment of the conditions caused by them [21]. Due to the repeated exposure of these Azole group of antibiotics, has led to the emergence of the azole resistant strains of Candida [22]. Apart from the repeated exposure of the azole group of antibiotics, point mutations of genes is also responsible for the azole resistance in Candida. Point mutations in MRR1 and TAC1 promotes the increased efflux of Azole, increases the expression of UPC2 throughout the ergosterol pathway, mutation in the ERG11 and ERG6 prevents the azole binding and the formation of the toxic sterols respectively [23].

Thus, in order to evaluate the alternate antimicrobials against the azole resistant strains of *C. albicans* an attempt has been made in this paper to evaluate their antimicrobial properties against these species.

2. Materials and Methods:

2.1Isolation and identification of *C. albicans* from Periodontitis cases:

2.1.1 Patient selection:

A total of 33 patients were identified from the Outpatient Department of Periodontics at I.T.S. Dental College, Hospital and Research Centre, Greater Noida. All the recruited patients were divided into: Healthy subjects (n=11) and Stage II Periodontitis group (n=11) and Stage III periodontitis group (n=11) based on the American Association of Periodontology classification 2017. Individuals who presented BOP, PPD≥ 4mm, CAL ≥ 1-2mm were included in the diseased groups. Absence of the above parameters constituted the healthy group. All the teeth were examined using a standard periodontal probe (UNC-15, Hu Friedy, Chicago, IL, USA) by a calibrated examiner. The individuals who had received any periodontal treatment in the past 6 months, presence of aggressive periodontitis, pregnant and lactating women, denture wearers, underlying systemic disease or an immunocompromised state like HIV, chronic pulmonary disease treated by inhaled corticoids, non-steroidal anti-inflammatory drugs or antibiotic therapy in the past 6 months were excluded from the study.

2.2Sample Collection:

After obtaining an informed consent from all the participants supragingival plaque and saliva was carefully removed with sterile gauze, the teeth were dried and subgingival biofilm samples were

acquired using sterile curettes from the deepest periodontal pocket with bleeding or from the healthy sulcus (no bleeding upon probing) of each subject, respectively and were stored at 4˚C in sterile saline blanks till further processing.

2.3Isolation and identification of *Candida*:

To isolate *Candida* species, the subgingival plaque samples were streaked on sterile plates of Sabourauds Dextrose Agar (SDA) followed by incubation at 37 °C for 48 hours [24]. In order to confirm the identity of the *C. albicans* the isolates obtained on the SDA plates, they were streaked on differential CHROM Agar (HiChrome™ *Candida* Differential Agar) for purification and morphological characterization of *C. albicans.* The inoculated plates were then incubated at 37˚ C for 4 days with constant monitoring for subsequent microbiological analysis. The isolated colonies from the SDA cultured plates were gram stained and observed under the oil immersion objective under the microscope for the morphological identification of *C. albicans*.

2.4Antifungal sensitivity test:

Antifungal sensitivity test of various Azole group of antibiotics was carried out as per the CLSI guidelines [25]. *Candida* was grown in BHIB overnight to attain the CFU of ~10^6 per ml. 100 µl of *Candida* was swabbed aseptically on Muller Hinton Agar plates and agar wells measuring 8 mm were punched with the help of sterilized microtips. The wells were loaded with 50 µl of Fluconazole, Itraconazole and Ketoconazole at the concentration of 50 µg/ml was added to the wells, and the plates were incubated at 37 °C for 48 hours.

2.5Isolation and identification of bacteria from the soil sample for the biosynthesis of silver nanoparticles:

1 gm of soil sample was diluted in 10 ml of sterile distilled water and was diluted serially to make the dilutions from 10^{-1} to 10^{-5}. 100 µl from each dilution was transferred into Nutrient Agar media and spread with the help of a glass spreader followed by incubation at 37°C for 24 hours after which the Colony Forming Units or CFU was evaluated [26]. The bacterial isolate thus obtained was labelled as NSCB-2, which was further investigated by using 16S rRNA molecular technique [27,28].

2.6Molecular characterization of the bacteria isolated from soil sample:

The identification of isolates was carried out at the sequencing facility of National Centre for Microbial Resource (NCMR), National Centre for Cell Science, Pune. At the facility, genomic DNA was isolated by the standard phenol/chloroform extraction method [29], followed by PCR amplification of the 16S rRNA gene using universal primers 16F27 [5'-CCA GAG TTT GAT CMT GGC TCA G-3'] and 16R1492 [5'-TAC GGY TAC CTT GTT ACG ACT T-3']. The amplified 16S rRNA gene PCR product was purified by PEG-NaCl precipitation and directly sequenced on an ABI® 3730XL automated DNA sequencer (Applied Biosystems, Inc., Foster City, CA) as per manufacturer's instructions. Essentially, sequencing was carried out from both ends using additional internal primers so that each position was read at least twice. Assembly was carried out using Lasergene package followed by identification using the EzBioCloud database [30]. Finally, data that were obtained from the sequencing process were Blast using BLASTn program available at the National Centre for Biotechnology Information (NCBI). The nucleotide sequence thus obtained of the NSB-2 bacterium was submitted to the NCBI database and Gen accession numbers were obtained. Also, the nucleotide sequences were further analyzed by MEGA 11 software for analysis of the evolutionary maximum likelihood.

3. Biosynthesis of silver nanoparticles from the bacteria isolated from the soil samples:

The isolate thus obtained were grown in 100 ml of sterile nutrient broth followed by the incubation in a shaker incubator at 200 rpm for 72 hours at 37°C [31]. Post incubation, the culture was centrifuged at 10,000 rpm for 20 minutes. 10 ml of the obtained supernatant was then mixed with 1mM $AgNO_3$ solution containing 0.017 gm of silver nitrate dissolved in 100 ml of distilled water out of which 10 ml was discarded and the remaining 90 ml was used for the biosynthesis of silver nanoparticles [32]. This reaction mixture was then incubated at room temperature for 48 hours. The obtained silver nanoparticles were centrifuged at 10,000 rpm for 15 minutes to separate the supernatant and pellet. The supernatant was discarded and the pellet collected was washed thrice with sterile distilled water and was recentrifuged again at 12,000 rpm for 20 minutes. This process was repeated thrice and the pellet obtained was oven dried at 65°C for 10 hours. The dried powder was collected and labelled as BNPs (Bacillus Silver Nanoparticles) and stored in a universal container and stored at 4°C for the characterization and antimicrobial assessment.

3.1Biosynthesis of Silver Nanoparticles from the Neem Leaf Extracts (NLNP):

0.017 gm of silver nitrate was dissolved in 100 ml of distilled water in order to prepare 1mM AgNO3 solution. 90 ml of the prepared solution was mixed with 10 ml of the ethanolic extract of Neem leaves [33,34]. The flask containing the reaction mixture was then immediately wrapped in Aluminum foil in order to prevent the photoactivation of the silver nanoparticles and it was incubated at the room temperature for 24 hours. Post incubation the color of the reaction mixture changed from pale yellow to brownish grey, indicating the production of silver nanoparticles. The obtained silver nanoparticles were centrifuged at 10,000 rpm for 15 minutes to separate the supernatant and pellet. The supernatant was discarded and the pellet collected was washed thrice with sterile distilled water and was recentrifuged again at 12,000 rpm for 20 minutes. This process was repeated thrice and the pellet obtained was oven dried at 65°C for 10 hours. The dried powder was collected and labelled as NLNPs (Neem Leaf Silver Nanoparticles) and stored in a universal container and stored at 4°C for the characterization and antifungal assessment.

3.2Polyethylene glycol capping of silver nanoparticles:

The PEG coating of the AgNPs was carried out based on the method of Kasim et al. [35] with slight modification. 30 gm of PEG (Sigma-Aldrich, Gillingham, UK), was dissolved in 120 mL of distilled water and stirred using a magnetic stirrer at medium speed for 24 h and room temperature [35,36]. Then, the PEG solution was mixed with a 50 mL of AgNPs solution and stirred using a magnetic stirrer at medium speed and room temperature for 48 hours as shown in **Fig. 1 (a)** and **(b)**.

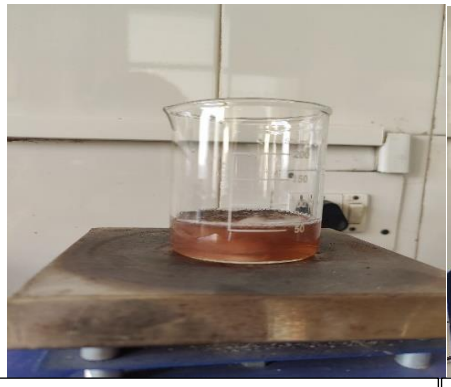

Fig. 1 (a) PEG Coating of NLNPs

Fig. 1 (b) PEG Coating of BNPs

3.3Characterization of silver nanoparticles:

The synthesized silver nanoparticles were scanned from 200-800 nm for detecting the Surface Plasmon Response parameter of the synthesized AISNPs on UV-Visible Spectrophotometer (Shimadzu UV-1800). The crystallinity of the nanoparticles was screened by XRD by using the Pan-Analytical (Netherlands) X'Pert PRO X-ray diffractometer and Cu-Kα radiation (λ=1.54059 Å) with an angular range of 20-80˚at 40kV and 30 mA. The powdered nanoparticle was mixed with KBr in a ratio of 1:100 and analyzed for the presence for various functional groups within the range of 500-4000 cm-1 through the FTIR. Size and surface morphology of the synthesized silver nanoparticles was done by dropping the sonicated nanoparticles on copper grids, which were dried and examined under the Transmission electron microscope (JEOL-JEM-1400) at 120kV accelerating voltage. The AISNPs were also analyzed for their hydrodynamic particle diameter through Dynamic Light Scattering and Zeta Potential analysis activity was proceeded through the Zeta Sizer instrument (Malvern, UK).

3.4Screening of antimicrobial activities of synthesized silver nanoparticles:

Antifungal activity of AgNPs were evaluated by the agar well diffusion method [37,38]. *C. albicans* was grown in BHIB overnight to attain the CFU of ~10^6 per ml. 100 µl of the growth obtained was spread on Muller Hinton Agar plates and five agar wells (8 mm) were punched with the help of sterilized microtips. The wells were loaded with 50 µl of BNPs, NLNPs, P-BNPs and P-NLNPs (P= PEG coated) having a concentration of 50 µg/ml. Amphotericin-B with the same concentration of 50 µg/ml was added to the well labelled as PC (Positive Control) and autoclaved distilled water was used as a negative control. The plates were incubated at 37˚C for 48 hours and the result was analyzed and tabulated, based on which the interpretation was deduced.

4. Result:

4.1Isolation and Identification of *Candida*:

33 systemically healthy subjects participated in the study out of which 22 subjects suffered from periodontitis while 11 subjects had a healthy periodontium. On the examination of the subgingival samples collected from the patients 18 out of 33 samples showed growth on SDA media after 24-48 hours (Fig. 2 a). These samples were Gram stained and checked under the microscope for the presence of *Candida* (Fig. 2 b). Notably, 4 out of 18 slides of the samples showed the presence of pseudo-hyphae which is an identification feature of *Candida* species. After a confirmatory culture on differential CHROM Agar Media, three out of four samples were positive for found to be positive for *C. albicans* (Fig. 2 c) which was further investigated for the antibiotic sensitivity test against the azole group of antifungal antibiotics.

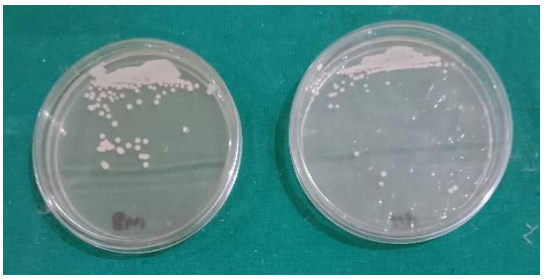

Fig. 2 (a) Isolation of *C. albicans* on SDA Plate

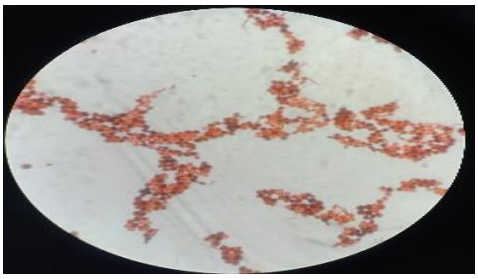

Fig. 2 (b) Staining Reaction of *C. albicans*

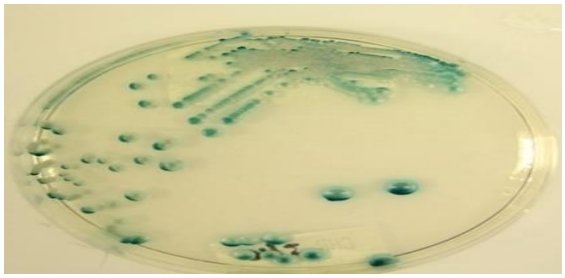

Fig. 2 (c) Isolation of *C. albicans* on CHROM Agar

4.2Anti-Fungal Susceptibility Test:

The samples were subjected to anti-fungal susceptibility test by Well-diffusion method as per the parameters of CLSI guidelines [25]. Limited zones of inhibition were seen around the wells containing Fluconazole (7 mm), Itraconazole (0 mm), Clotrimazole (0 mm) and Ketoconazole (0 mm). According to the diameter of the ZOI obtained from the results it was evident to conclude that the isolated species of *C. albicans* was resistant to all the three anti-fungal agents (Fig. 3).

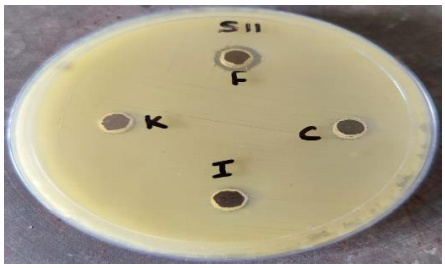

Fig. 3. Antifungal Susceptibility Test of antibiotics on *C. albicans* against fungal antibiotics Ketoconazole (K), Fluconazole (F), Itraconazole and Clotrimazole (C).

4.3Isolation and selection of silver nanoparticle producers:

Serially diluted soil suspension on nutrient agar plates were allowed to grow for 24 h at 37°C produced 3 different bacterial colonies. These 3 bacterial isolates were then grown on the nutrient agar media supplemented with 1 mM of $AgNO_3$ solution and incubated at 37°C for 24 hours. Only one bacterial strain was found to have the ability to grow on the $AgNO_3$ supplemented nutrient agar and was designated as strain NSB-1.

4.4Morphological and Biochemical characterization of the isolated bacteria from soil sample:

Based on the Gram staining, the morphology of the isolated bacteria was found to be Gram negative bacilli and were displayed as small pinpointed mucoidal colonies on nutrient agar media.

4.5Molecular identification of soil isolate *Klebsiella spp*.:

Based on the molecular identification of the bacteria by 16S rRNA identification, the bacterium was identified as *Klebsiella pneumoniae* subsp. q*uasipneumoniae*. The Gene accession number OP596438 was obtained after the submission of the nucleotide sequence to the NCBI. The evolutionary history was inferred by using the Maximum Likelihood method and Kimura 2-parameter model [39]. The tree with the highest log likelihood (-1949.00) is shown in Fig. 4. The percentage of trees in which the associated taxa clustered together is shown next to the branches. Initial tree(s) for the heuristic search were obtained automatically by applying Neighbor-Join and BioNJ algorithms to a matrix of pairwise distances estimated using the Maximum Composite Likelihood (MCL) approach, and then selecting the topology with superior log likelihood value.

The tree is drawn to scale, with branch lengths measured in the number of substitutions per site. This analysis involved 6 nucleotide sequences. Codon positions included were 1st+2nd+ 3rd+ Noncoding. There were a total of 1389 positions in the final dataset. Evolutionary analyses were conducted in MEGA11 [40].

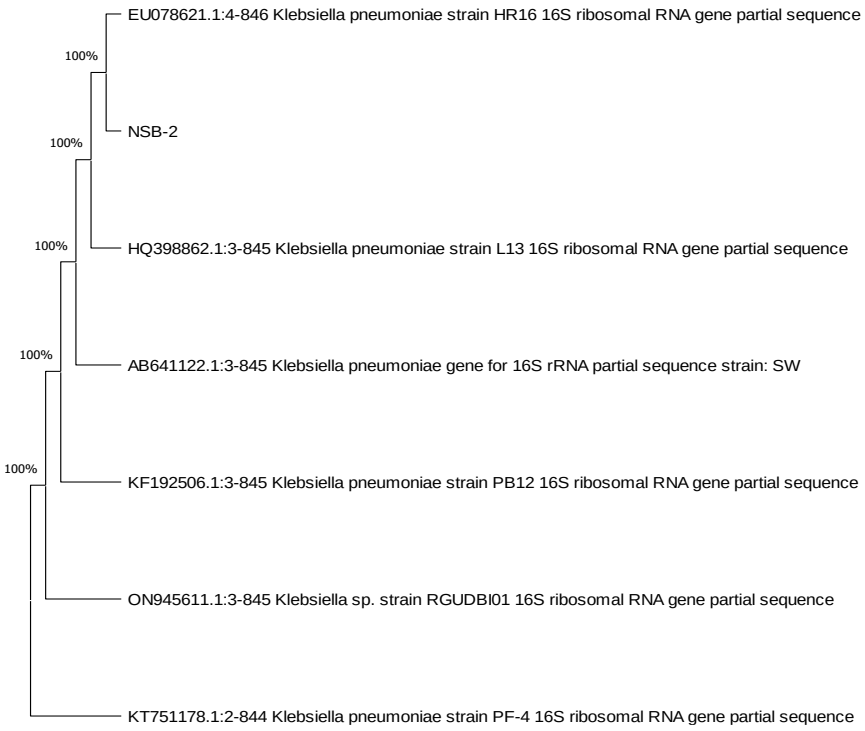

Fig. 4. Phylogenetic Tree of NSB-2 demonstrates its Maximum Likelihood with *K. pneumoniae* strain.

4.6Biogenic Synthesis of Silver Nanoparticles:

Nanoparticle formation was detected by the development of dark brown coloration of the solution, which was the resulted due to the reduction of 1mM $AgNO_3$ after the addition of ethanolic extract of Neem leaves and bacterial cellular extracts indicating the bio-reduction of Ag^+ to Ag^0, indicating the effect of surface plasmon resonance as shown in **Fig. 5 (a)** and **(b)**.

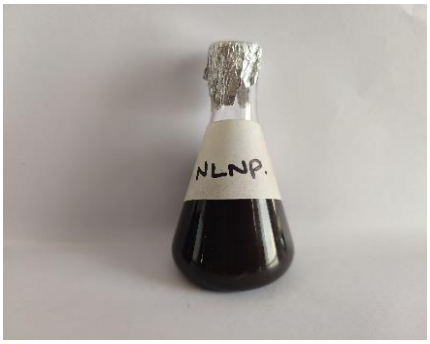

Fig. 5 (a) Biosynthesis of NLNP

Fig. 5 (b) Biosynthesis of BNP

4.7Characterization of Silver Nanoparticles:

A. UV-Visible spectrophotometry:

The surface plasmon resonance activity of BNP was noticed with the addition of cellular extracts of *Klebsiella spp.* to 1mM $AgNO_3$ solution which changes the color from pale yellow to brown after the incubation. Similar type of reaction was also noticed on the addition of the ethanolic extracts of Neem leaves to the 1mM $AgNO_3$ solution. The surface plasmon resonance observed in case of BNP was at 422.5 nm while in case of NLNP, the peak was observed at 432 nm, both of which were detected by the UV Visible spectroscopy as shown in **Fig. 6 (a)** and **(b)**. One of the key parameters that lead to the change in color of the silver nitrate solution to silver nanoparticles is due to the ability of the ethanolic extracts to act as a bio-reductant, in case of NLNPs and Bacterial cellular extract,

promoted the conversion of Ag^{+} to Ag^{0}. The peak intensity of BNPs and NLNPs obtained on the UV Visible spectrophotometer, thus indicated the formation of silver nanoparticles.

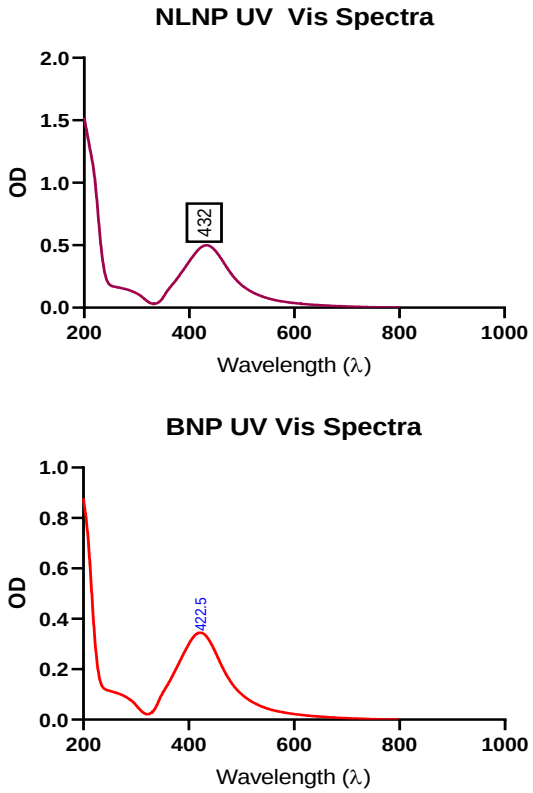

Fig. 5 (a) and (b). UV-Visible Spectroscopy analysis of NLNP and BNP Silver Nanoparticles.

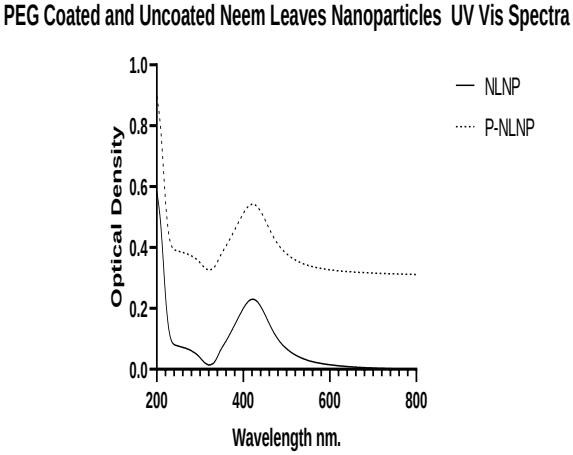

Fig. 6 (a)

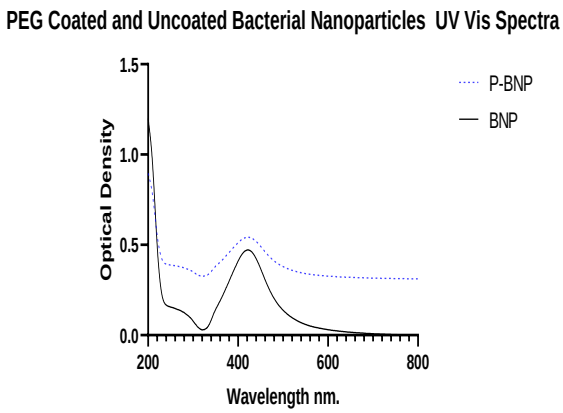

Fig. 6 (b)

Fig. 6 (a) and (b). UV-Visible Spectroscopy analysis of PEG coated and uncoated NLNP and BNP Silver Nanoparticles: P-NLNP =PEG coated Neem Leaf Nanoparticles, P-BNP= PEG coated Bacterial Nanoparticles, NLNP = Neem Leaf Nanoparticles and BNP = Bacterial Nanoparticles.

B. XRD:

Analysis of various angular diffraction patterns obtained after the analysis of the powdered AgNPs on XRD was then analyzed by using the software X'Pert Highscore Plus (Version 3.0, PANalytical, Netherlands). The result thus obtained was used for the calculation of the crystalline nature of the nanoparticles and also the various parameters like peaks, Full Wavelength Half Maxima (FWHM) and Miller's indices for the estimation of crystallinity of both BNPs as well as NLNPs. The diffraction peaks were received at 2θ of 38.1˚ (1 1 1), 44.2˚ (2 0 0), 64.5˚ (2 2 0) and 77.4˚ (3 1 1) were obtained in case of NLNPs crystallographic planes, respectively as shown in **Fig. 7 (a)**.

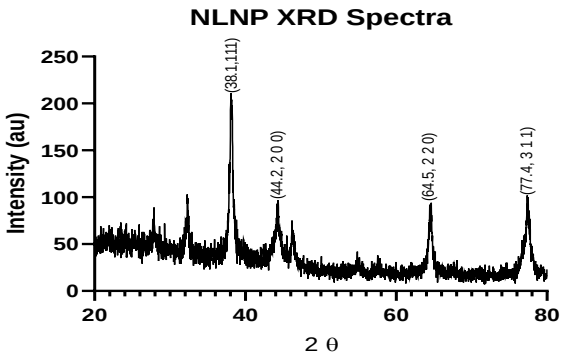

Fig. 7. (a) XRD Spectra of NLNP

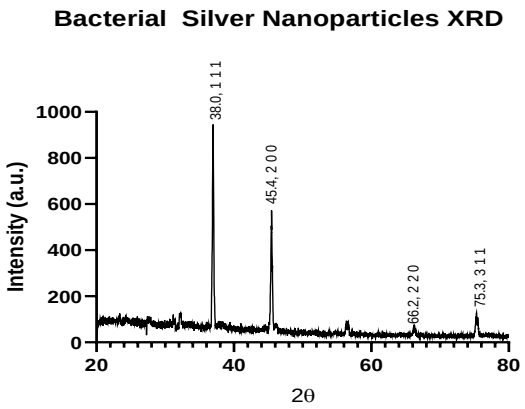

Fig. 7. (b) XRD Spectra of BNP

In case of BNPs, the peaks were obtained at 2θ of 38.0° (1 1 1), 45.4° (2 0 0), 66.2° (2 2 0) and 75.3° (3 1 1) were obtained as shown in **Fig. 7 (b)**. Analysis of the data obtained from the crystal patterns of both BNP and NLNP revealed the similarity of Face Centered Cubic shape.

C. Dynamic Light Scattering and Zeta Potential:

Hydrodynamic nanometer and ζ potential of BNP and NLNP were analyzed on Malvern Zetasizer. The AgNPs in the concentration of 100 µg/ml was dispersed in sterile double distilled water and the potential as well as the size of the nanoparticles were analyzed on the Zetasizer instrument. The mean of ζ potential of BNP was found to be -27.9 mV, while the size was 70.31 nm and the PDI value was 1.000. as shown in **Fig. 8 (a)** and **(b)**. In case of NLNP, the potential was found to be -19.7 mV and the size was 95.75 nm with the PDI value of 0.572, details of which is shown in **Fig. 8 (c)** and **(d)**. The values of PDI, thus obtained indicates that the nanoparticle solutions thus formed is monodispersed.

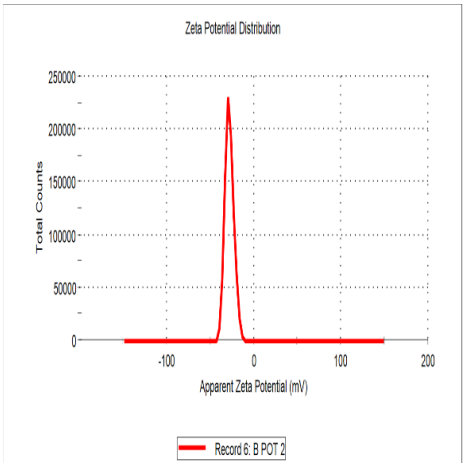

Fig. 8 (a) Zeta Potential of BNP

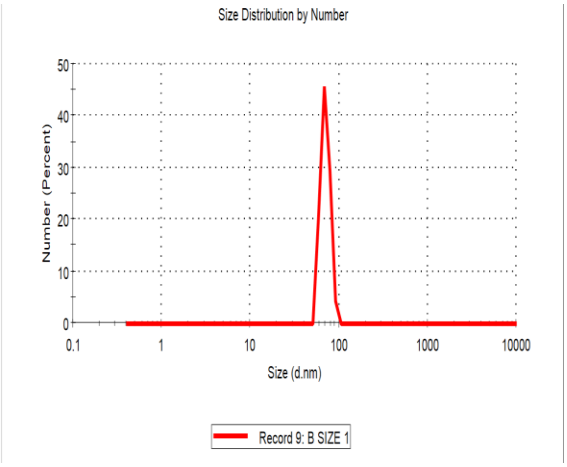

Fig. 8 (b) Zeta size of BNP

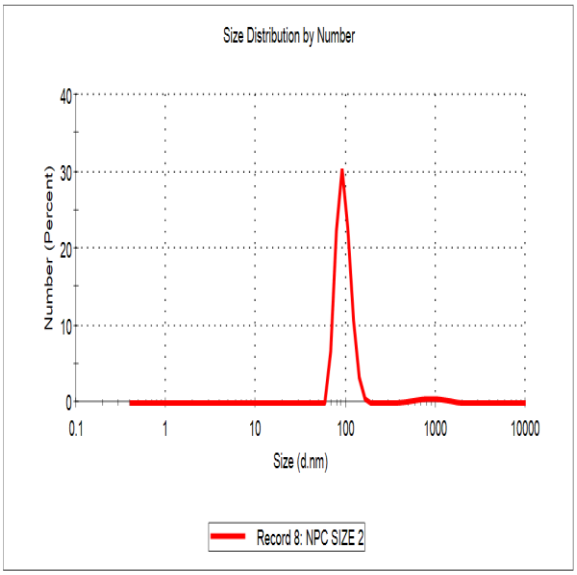

Fig. 8 (c) Zeta size of NLNP

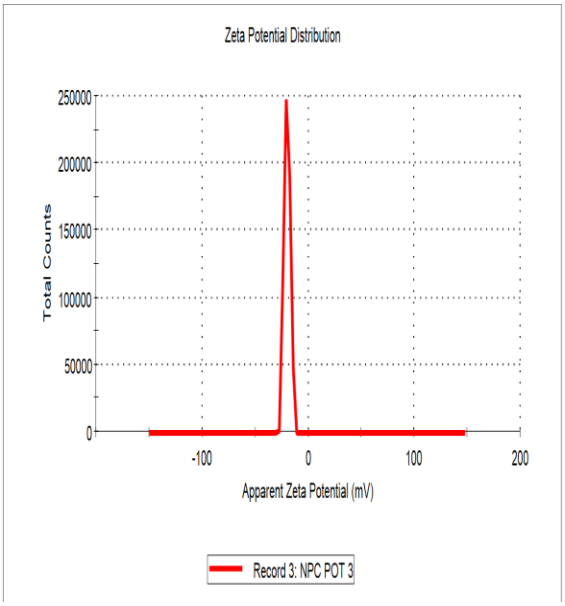

Fig. 8 (d) Zeta Potential of NLNP

D. FTIR:

To assess the presence of various biomolecules the BNP and NLNPs were analyzed through Fourier Transformed Infrared Spectroscopy. Peaks were observed at 3730.2, 3432.6, 2926.6, 1821.4, 1491.9, 1384.9, 1064.1 and 910.9 Wavenumbers (cm^{-1}) as shown in case of NLNP as shown in **Fig. 9 (a)**. The trough peaks at 3432.6 displayed the presence of OH groups along with Carbohydrates, Proteins and Phenols, whereas the peaks at 2926.6 displayed the presence of CH and CH_2 aliphatic stretching. The band stretches at 1491.9, 1384.9, 1064.1 and 910.9 displayed the presence of weak C=C bonds, C-H bends of alkanes, strong C-F stretching and unsubstituted Alkenes respectively. While in case of BNPs the peaks were noticed at 3435, 2993.7, 2956.2, 1892.4, 1650.7, 1487.9, 1441.6, 1218.1 and 948.4 wavenumbers (cm^{-1}) as shown in **Fig. 9 (b)**. The predominating type functional groups noticed were in the regions of 3095-2995, which indicated the presence of C-H stretch, indicating the presence of Aryl group. The region from 1487.9 lies in the region of C-C stretch, which indicates the presence of ring like structure. The Aryloxy C-O stretch is detected in the region between 1245-1200. The presence of these bonds along with the BNPs and NLNPs indicated the bonding of the chemo-constituents of the bacterial supernatant and neem leaf extracts that may have assisted in the biological reduction of Ag^+ to Ag^0, thus assisting in the formation of AgNPs.

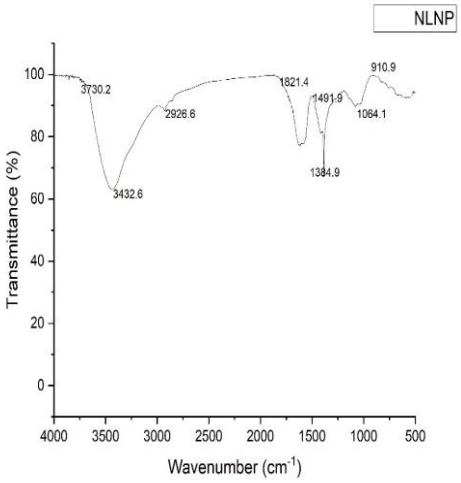

Fig. 9 (a) FTIR Spectra of NLNP

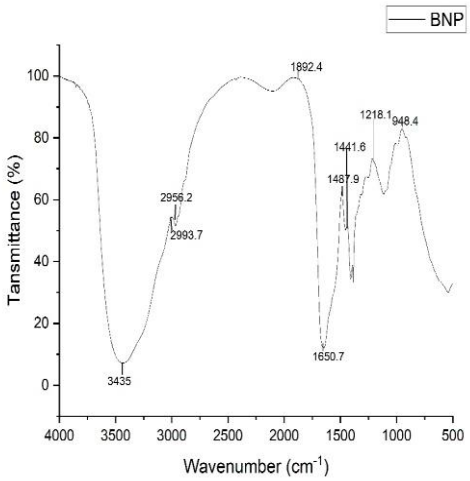

Fig. 9 (b) FTIR Spectra of BNP

E. Transmission Electron Microscopy Analysis:

TEM analysis of the BNPs depicted the presence of the spherical silver nanoparticles and the mean diameter of the synthesized nanoparticles was found to be around 19.02 nm, which was calculated by the ImageJ software (Version 1.80, USA). the result of which is as displayed in **Fig. 10 (a-d)**.

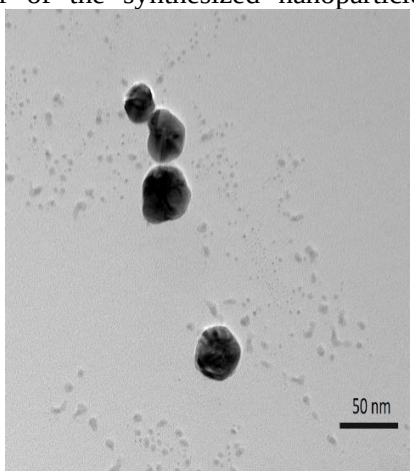

Fig. 10. (a) PEG uncoated BNPs

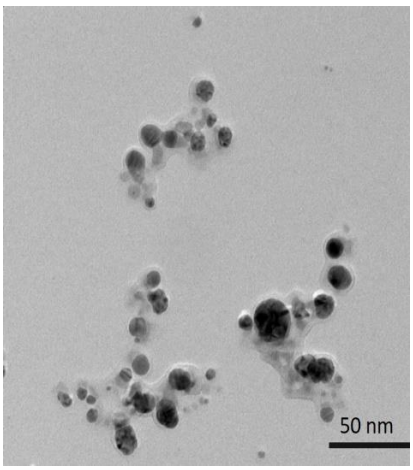

Fig. 10. (b) PEG coated BNPs

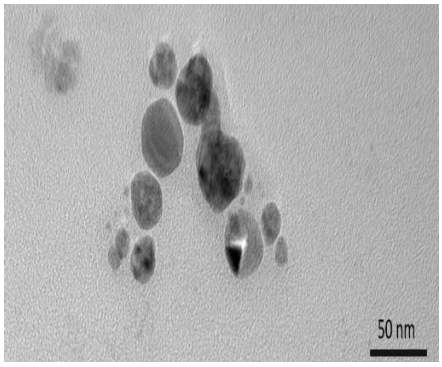

Fig. 10. (c) PEG uncoated NLNPs

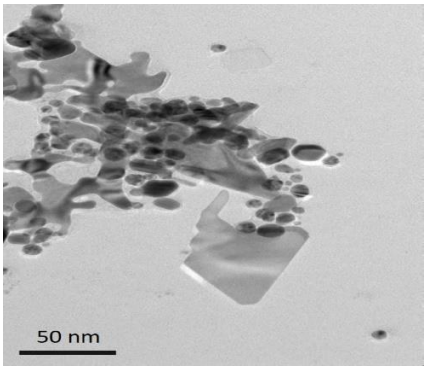

Fig. 10. (d) PEG coated NLNPs

4.8Assessment of Antimicrobial Sensitivity of AgNPs against Azole resistant *C. albicans*:

The Antimicrobial activity of BNP and NLNP was assessed by the well diffusion method (**Fig. 11**) against multi-drug resistant *C. albicans*. 50 µl of BNP, NLNP and PEG coated P-BNP and P-NLNPs were added to each well, which were punched on Muller Hinton Agar plates. The plates were then incubated at 37 °C for 48 hours and the zone of inhibition was assessed for the zone of inhibitions which was measured in 'mm' and the interpretation of the result was made.

It was observed that the zone of inhibition in case of non-coated BNP and NLNP against *C. albicans* was 20.1 and 18.7 respectively. While in case of PEG coated P-BNP and P-NLNP were 18.2 and 18 mm respectively. The results were compared with the standard anti-fungal antibiotic Fluconazole, with the concentration of 50 µg/ml, which showed the zone of inhibition of 0 mm against *C. albicans*.

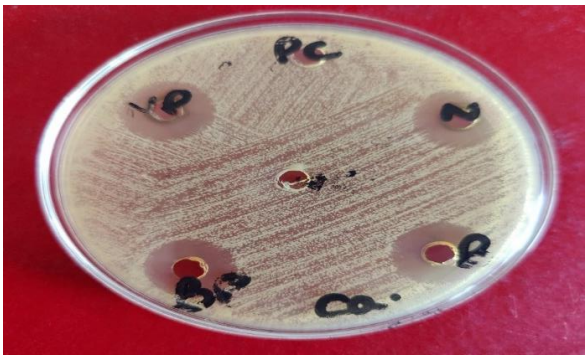

Fig. 11. Antifungal activity of PEG Coated Bacterial and Neem Leaf Nanoparticles (BP and NP) and uncoated nanoparticles (B and N) against *C. albicans*. PC= Positive Control, Fluconazole (50 µg/ml)

5. Conclusion:

C. albicans is a common type of oral pathogen that has been repeatedly found to be associated with Periodontitis cases worldwide [5,6]. The problem arises when the associated pathogens are reported for their drug resistance, that worsens the matter [23]. In order to tackle the anti-fungal resistance of *C. albicans* against various types of anti-fungal antibiotics, this study makes an attempt to find the alternate cure that has a strong potential to eliminate the pathogens. From the experiments conducted in this study, two types of nanoparticles of biogenic origin, i.e., made from the soil bacteria, *Klebsiella spp*. (BNP) and the other from Neem Leaf Extracts (NLNP), were treated against the *C. albicans* that were isolated from the patients suffering from chronic periodontitis. Also, it was checked that whether the addition of any capping reagent like PEG or Polyethylene Glycol's addition can impact the anti-fungal property of these nanoparticles.

It can be concluded from the study that both the nanoparticles i.e., BNP and NLNPs were equally potent against Azole resistant *C. albicans*. It was also noted that when both of these nanoparticles when capped with PEG has comparatively less anti-fungal activity as compared to the uncapped nanoparticles.

6. Acknowledgements:

The authors are thankful to the I.T.S. Dental College, Hospital and Research Centre, Greater Noida for their kind support and assistance to carry this study. We are also grateful to IIT-Delhi for providing the technical assistance and permitting to utilize their XRD and FTIR facilities, which were the utmost requirement for the analysis of nanoparticles. Also, we are thankful to A.I.I.M.S, New Delhi for providing the facilities of Transmission Electron Microscopy and Zeta Sizer for the imaging and estimation of size and potential of the nanoparticles.

7. References:

1. Unniachan AS, Jayakumari NK, Sethuraman S. Association between Candida species and periodontal disease: A systematic review. Curr Med Mycol. 2020;6(2):63–8.
2. Page RC, Eke PI. Case Definitions for Use in Population-Based Surveillance of Periodontitis. J Periodontol. 2007;78(7s): 1387–99.

3. Canabarro A, Valle C, Farias MR, Santos FB, Lazera M, Wanke B. Association of subgingival colonization of Candida albicans and other yeasts with severity of chronic periodontitis. J Periodontal Res. 2013;48(4): 428–32.
4. Alnuaimi AD, Wiesenfeld D, O'Brien-Simpson NM, Reynolds EC, McCullough MJ. Oral Candida colonization in oral cancer patients and its relationship with traditional risk factors of oral cancer: A matched case-control study. Oral Oncol [Internet]. 2015;51(2):139–45. Available from: http://dx.doi.org/10.1016/j.oraloncology.2014.11.008
5. Sen BH, Meurman JH, Diseases M, Faculty D. Y Easts in a Pical P Eriodontitis. Crit Rev Oral Biol Med. 2003;14(2):128–37.
6. Shettar L, Thakur SL, Surgeon D. Detection of Candida Albicans and its Adherence to Epithelial Cells in Periodontal Health and Disease – A Clinicomicrobiological Study. Ann RSCB. 2021;25(3).
7. Sardi JCO, Duque C, Mariano FS, Marques MR, Höfling JF, Gonçalves RB. Adhesion and invasion of Candida albicans from periodontal pockets of patients with chronic periodontitis and diabetes to gingival human fibroblasts. Med Mycol. 2012;50(1):43–9.
8. Sardi JCO, Duque C, Mariano FS, Peixoto ITA, Höfling JF, Gonçalves RB. Candida spp. in periodontal disease: a brief review. J Oral Sci. 2010;52(2):177–85.
9. Kıvanç M, Er S. Biofilm formation of candida spp. Isolated from the vagina and antibiofilm activities of lactic acid bacteria on the these candida isolates. Afr Health Sci. 2020;20(2):641–8.
10. Kumar D, Muralidhar S, Banerjee U, Basir S, Khan L. Antifungal Resistance Patterns, Virulence Attributes and Spectrum of Oral Candida Species in Patients with Periodontal Disease. Br Microbiol Res J. 2015;5(1):68–75.
11. Jewtuchowicz VM, Mujica MT, Malzone MC, Cuesta A, Nastri ML, Iovannitti CA, et al. Genetic relatedness of subgingival and buccal Candida dubliniensis isolates in immunocompetent subjects assessed by RAPD-PCR. J Oral Microbiol. 2009;1(2009).
12. Urzua B, Hermosilla G, Gamonal J, Morales-Bozo I, Canals M, Barahona S, et al. Yeast diversity in the oral microbiota of subjects with periodontitis: Candida albicans and Candida dubliniensis colonize the periodontal pockets. Med Mycol. 2008;46(8):783–93.
13. Filler SG, Pfunder AS, Spellberg BJ, Spellberg JP, Edwards JE. Candida albicans stimulates cytokine production and leukocyte adhesion molecule expression by endothelial cells. Infect Immun. 1996;64(7):2609–17.
14. Machado AG, Komiyama EY, Soléo S, Cardoso AO, Brighenti FL, Koga-ito CY. From Patients With Chronic Periodontitis. J Appl Oral Sci. 2010;384–7.
15. Krogh P. The role of yeasts in oral cancer by means of endogenous nitrosation. Acta Odontol Scand. 1990;48(1):85–8.
16. Sardi JCO, Almeida AMF, Mendes Giannini MJS. New antimicrobial therapies used against fungi present in subgingival sites - A brief review. Arch Oral Biol. 2011;56(10): 951–9.
17. Radunovic M, Barac M, Pficer JK, Pavlica D, Jovanovic A, Pucar A, et al. Antifungal Susceptibility of Candida albicans Isolated from Tongue and Subgingival Biofilm of Periodontitis Patients. Antibiotics. 2022;11 (6):1–13.
18. Castelo-Branco DSCM, Brilhante RSN, Paiva MAN, Teixeira CEC, Caetano EP, Ribeiro JF, et al. Azole-resistant Candida albicans from a wild Brazilian porcupine (Coendou prehensilis): A sign of an environmental imbalance? Med Mycol. 2013;51(5):555–60.
19. Bhattacharya S, Esquivel BD, White TC. Overexpression or deletion of ergosterol biosynthesis genes alters doubling time, response to stress agents, and drug susceptibility in Saccharomyces cerevisiae. MBio. 2018;9(4).
20. Delattin N, Cammue BP, Thevissen K. Reactive oxygen species-inducing antifungal agents and their activity against fungal biofilms. Future Med Chem. 2014;6(1):77–90.
21. Sobel JD, Sobel R. Current treatment options for vulvovaginal candidiasis caused by azole-resistant Candida species. Expert Opin Pharmacother [Internet]. 2018;19(9):971–7. Available from: https://doi.org/10.1080/14656566.2018.1476490
22. Sanglard D, Kuchler K, Ischer F, Pagani JL, Monod M, Bille J. Mechanisms of resistance to azole antifungal agents in Candida albicans isolates from AIDS patients involve specific multidrug transporters. Antimicrob Agents Chemother. 1995;39(11):2378–86.
23. Bhattacharya S, Sae-Tia S, Fries BC. Candidiasis and mechanisms of antifungal resistance. Antibiotics. 2020;9(6):1–19.
24. Petrović SM, Cimbaljević M, Radunović M, Pfićer JK, Jotić A, Pucar A. Detection and sampling methods for isolation of Candida spp. from oral cavities in diabetics and non-

diabetics. Braz Oral Res. 2015;29(1):1–7.
25. Clinical and Laboratory Standards Institute. Clinical and Laboratory Standards Institute (CLSI). Performance Standards for Antimicrobial Susceptibility Testing. 30th ed. CLSI Suppl M100. 2020;
26. Das VL, Thomas R, Varghese RT, Soniya E V., Mathew J, Radhakrishnan EK. Extracellular synthesis of silver nanoparticles by the Bacillus strain CS 11 isolated from industrialized area. 3 Biotech. 2014;4(2):121–6.
27. Skariyachan S, Rao AG, Patil MR, Saikia B, Bharadwaj Kn V, Rao Gs J. Antimicrobial potential of metabolites extracted from bacterial symbionts associated with marine sponges in coastal area of Gulf of Mannar Biosphere, India. Lett Appl Microbiol. 2014;58(3):231–41.
28. Leslie VA, Mohammed Alarjani K, Malaisamy A, Balasubramanian B. Bacteriocin producing microbes with bactericidal activity against multidrug resistant pathogens. J Infect Public Health [Internet]. 2021;14(12):1802–9. Available from: https://doi.org/10.1016/j.jiph.2021.09.029
29. Sambrook J, Fritsch EF, Maniatis T. Molecular Cloning a laboratory manual. New York: Cold Spring Harbor Laboratory Press; 1989.
30. Yoon SH, Ha SM, Kwon S, Lim J, Kim Y, Seo H, et al. Introducing EzBioCloud: A taxonomically united database of 16S rRNA gene sequences and whole-genome assemblies. Int J Syst Evol Microbiol. 2017;67(5):1613–7.
31. Shanthi S, David Jayaseelan B, Velusamy P, Vijayakumar S, Chih CT, Vaseeharan B. Biosynthesis of silver nanoparticles using a probiotic Bacillus licheniformis Dahb1 and their antibiofilm activity and toxicity effects in Ceriodaphnia cornuta. Microb Pathog [Internet]. 2016;93:70–7. Available from: http://dx.doi.org/10.1016/j.micpath.2016.01.014
32. Pourali P, Yahyaei B. Biological production of silver nanoparticles by soil isolated bacteria and preliminary study of their cytotoxicity and cutaneous wound healing efficiency in rat. J Trace Elem Med Biol [Internet]. 2016;34:22–31. Available from: http://dx.doi.org/10.1016/j.jtemb.2015.11.004
33. Senthilkumar P, Rashmitha S, Veera P, Vijay Ignatious C, SaiPriya C, Samrot A V. Antibacterial activity of neem extract and its green synthesized silver nanoparticles against pseudomonas aeruginosa. J Pure Appl Microbiol. 2018;12(2):969–74.
34. Khan K, Javed S. Silver nanoparticles synthesized using leaf extract of Azadirachta indica exhibit enhanced antimicrobial efficacy than the chemically synthesized nanoparticles: A comparative study. Sci Prog. 2021;104(2):1–15.
35. Kasim ASM, Ariff A Bin, Mohamad R, Wong FWF. Interrelations of synthesis method, polyethylene glycol coating, physico-chemical characteristics, and antimicrobial activity of silver nanoparticles. Nanomaterials. 2020;10(12):1–15.
36. Xiu ZM, Zhang QB, Puppala HL, Colvin VL, Alvarez PJJ. Negligible particle-specific antibacterial activity of silver nanoparticles. Nano Lett. 2012;12(8):4271–5.
37. Ramzan M, Karobari MI, Heboyan A, Mohamed RN. Synthesis of Silver Nanoparticles from Extracts of Wild Ginger (Zingiber zerumbet) with Antibacterial Activity against Selective Multidrug Resistant Oral Bacteria. 2022;
38. Mohamed DS, El-Baky RMA, Sandle T, Mandour SA, Ahmed EF. Antimicrobial activity of silver-treated bacteria against other multi-drug resistant pathogens in their environment. Antibiotics. 2020;9(4).
39. Kimura M. A simple method for estimating evolutionary rates of base substitutions through comparative studies of nucleotide sequences. J Mol Evol. 1980;16(2):111–20.
40. Tamura K, Stecher G, Kumar S. MEGA11: Molecular Evolutionary Genetics Analysis Version 11. Mol Biol Evol. 2021;38(7):3022–7.